HHS Public Access

Author manuscript

Ann N Y Acad Sci. Author manuscript; available in PMC 2021 January 01.

Published in final edited form as:

Ann N Y Acad Sci. 2020 January ; 1460(1): 57–67. doi:10.1111/nyas.14250.

Cells from a GDF5 origin produce zonal tendon-to-bone attachments following anterior cruciate ligament reconstruction

Yusuke Hagiwara[1,2], **Felix Dyrna**[3], **Andrew F. Kuntz**[4], **Douglas J. Adams**[5,6], **Nathaniel A. Dyment**[4]

[1]Department of Orthopaedic Surgery, Inada Hospital, Nara Prefecture, Japan.

[2]Department of Orthopaedic Surgery, Nara Medical University, Nara Prefecture, Japan.

[3]Department of Trauma, Hand, and Reconstructive Surgery, University Hospital Münster,Münster, Germany.

[4]McKay Orthopaedic Research Laboratory, Department of Orthopaedic Surgery, University of Pennsylvania, Philadelphia, Pennsylvania.

[5]Department of Orthopedics, University of Colorado Anschutz Medical Campus, Aurora, Colorado.

[6]Department of Reconstructive Sciences, UConn Health, Farmington, Connecticutt.

Abstract

Following anterior cruciate ligament (ACL) reconstruction surgery, a staged repair response occurs where cells from outside the tendon graft participate in tunnel integration. The mechanisms that regulate this process including the specific cellular origin are poorly understood. Embryonic cells expressing growth and differentiation factor 5 (GDF5) give rise to several mesenchymal tissues in the joint and epiphyses. We hypothesized that cells from a GDF5 origin, even in the adult tissue, would give rise to cells that contribute to the stages of repair. ACLs were reconstructed in *Gdf5-Cre*;R26R-tdTomato lineage tracing mice to monitor the contribution of *Gdf5-Cre*;tdTom$^+$ cells to the tunnel integration process. Anterior–posterior drawer tests demonstrated 58% restoration in anterior–posterior stability. *Gdf5-Cre*;tdTom$^+$ cells within the epiphyseal bone marrow adjacent to tunnels expanded in response to the injury by 135-fold compared with intact controls to initiate tendon-to-bone attachments. They continued to mature the attachments yielding zonal insertion sites at 4 weeks with collagen fibers spanning across unmineralized and mineralized fibrocartilage and anchored to the adjacent bone. The zonal attachments possessed tidemarks with concentrated alkaline phosphatase activity similar to native entheses. This study established that mesenchymal cells from a GDF5 origin can contribute to zonal tendon-to-bone attachments within bone tunnels following ACL reconstruction.

Address for correspondence: Nathaniel A Dyment, McKay Orthopaedic Research Laboratory, Department of Orthopaedic Surgery, University of Pennsylvania, 330A Stemmler Hall, 3450 Hamilton Walk, Philadelphia, PA 19104-6081. dyment@pennmedicine.upenn.edu.

Author contributions

Y.H., F.D., A.F.K., D.J.A., and N.A.D. designed experiments. Y.H. and N.A.D. performed experiments. Y.H., F.D., A.F.K., D.J.A., and N.A.D. analyzed data. Y.H., F.D., A.F.K., D.J.A., and N.A.D. wrote the manuscript.

Competing interests

The authors declare no competing interests

Graphical abstract

The objective of this study was to use *Gdf5-Cre* transgenic mice to trace the origin of cells that revitalize the tendon graft following ACL reconstruction in a mouse model and to examine the extent to which these cells can create mineralized attachments within bone tunnels.

Keywords

anterior cruciate ligament; growth and differentiation factor 5; lineage trace; tendon-to-bone repair

Introduction

Approximately 30% of U.S. adults suffer from tendon and ligament injuries[1]. These injuries frequently occur near insertion sites into bone (i.e., entheses) and do not spontaneously heal[2,3]. Traditional tendon-to-bone repair, where the tendon is reattached to the underlying bone with sutures, does not create a zonal enthesis with collagen fibers spanning across unmineralized and mineralized fibrocartilage. On the other hand, ligament reconstructions where a tendon graft is placed through bone tunnels often do produce zonal attachments. Therefore, a better understanding of the mechanisms that drive zonal tendon-to-bone attachments following ligament reconstructions may be informative to more severe tendon enthesis repairs, such as those to the rotator cuff tendons.

Anterior cruciate ligament (ACL) reconstruction is the most common ligament reconstruction procedure, accounting for approximately 250,000 annually in the United States alone[4]. The annual costs of MRI, surgery, bracing and rehabilitation are estimated to exceed 2 billion dollars. Additionally, indirect costs such as lost wages, decreased productivity, and disability are substantial[4]. The highest injury prevalence is in young adult patients, typically athletes. Return to sport following ACL injury, reconstruction, and rehabilitation often exceeds 8 months[5]. Therefore, there is a clinical desire to expedite this process through novel treatment strategies.

Multiple stages of healing have been classified following ACL reconstruction[6–13], including (1) endogenous cell death leading to a degeneration of the graft, (2) vascularization and revitalization of the graft when new blood vessels and fibroblasts repopulate the graft, and (3) ligamentization of the graft where the infiltrated cells remodel the extracellular matrix and take on a ligament-like phenotype. In addition, cells that revitalize the graft also anchor the graft to bone adjacent to the tunnels via zonal tendon-to-bone insertion sites. Similar to enthesis embryonic development[14], the desired tendon-to-bone insertion healing process will involve the synthesis of collagen fibers that will need to be anchored to the underlying bone matrix, and then the cells within this matrix will need to produce unmineralized and mineralized fibrocartilage to create a zonal insertion site.

Specific markers that identify the origin of cells that contribute to the tunnel integration following ACL reconstruction are limited. Rodent models can assist in identifying these cells and elucidating the biological mechanisms that govern the formation of a zonal tendon-to-bone insertion site during adult repair. For instance, a rat femoral tunnel implant model

using non-GFP allografts into GFP recipients demonstrated clearly that cell populations from outside the graft drive tunnel integration[7], which was later confirmed in a rabbit GFP allograft model[15]. ACL reconstruction procedures in mice have been established[16–19], which opens up the possibility of using powerful genetic tools found in various mouse strains to better define the cellular origin and molecular regulation of tendon-to-bone repair.

Growth and differentiation factor 5 (GDF5) is a cell signaling ligand that is part of the TGF-β superfamily. It is a key signaling molecule in the formation of joints[20] as it is one of the earliest markers to identify the interzone cells that give rise to tissues in the joint. In addition, it regulates secondary ossification[21] and is expressed by progenitors that give rise to osteogenic cells within the secondary ossification center. While these cells lose GDF5 expression after birth[21], their progeny persist into adulthood, giving rise to trabecular bone within the epiphyses[22]. Since mesenchymal cells within the joint and epiphysis originate from a GDF5 origin, this marker could be used to trace cell populations that contribute to ACL graft repopulation and tunnel integration. Therefore, the objective of this study was to use *Gdf5-Cre* transgenic mice to trace the origin of cells that revitalize the tendon graft following ACL reconstruction in a mouse model and to examine the extent to which these cells are capable of creating mineralized attachments within the bone tunnels.

Materials and methods

Mouse models

***Gdf5-Cre*;R26R-tdTomato.—**Constitutive *Gdf5-Cre* mice[22,23] were crossed with Ai9 R26R-tdTomato Cre reporter mice (B6;129S6-Gt(ROSA)26Sor$^{tm9(CAG-tdTomato)Hze}$/J, Jackson Laboratory) to label mesenchymal cells within the joints and epiphyses to monitor revitalization of ACL grafts following reconstruction.

Experimental design

Three- to four-month-old mice were used in this study. Three groups were created for anterior-posterior drawer mechanical assessment to establish the stability of the knee in this new model: ACL reconstructed knee (reconstructed ACL: ACLR) ($n = 8$), ACL-deficient knee (transected ACL (ACLT)) ($n = 9$), or intact knee ($n = 9$). The animals were assessed at 4 weeks postsurgery. Eight additional mice were subjected to ACL reconstruction and the bone tunnel regions were examined using multiplexed mineralized cryohistology at 1 week ($n = 3$) and 4 weeks ($n = 5$) postsurgery. These mice received an intraperitoneal (IP) injection of demeclocycline (30 μg/g) 1 day prior to sacrifice to label deposited mineral.

Unilateral murine ACL reconstruction procedure using tail tendon autograft

All mice were approved by the UConn Health Institutional Animal Care and Use Committee. Mice were anesthetized, sterilely prepped, and the surgery was conducted similarly to previous work[19]. Three small incisions (3 mm each, spaced ~30 mm apart) were made in the tail to access the tail tendons (Fig. 1A). Continuous tail tendon bundles (3–4 tendons in each bundle) were then identified and removed (5–6 cm in length) (Fig. 1B). Suture was passed through a small length of 25G needle (3-mm long) to create a cortical fixator which was then passed over the tail tendon bundle (yellow arrowhead in Fig. 1C).

Nylon suture was tied around the tendons at each end of the bundle (green circle in Fig. 1C) and then the bundle was submerged in PBS until the tunnels were drilled. The knee joint space was accessed via an anteromedial approach (Fig. 1D) and the ACL was transected near its femoral insertion with a 28G needle. A manual drawer test was performed to confirm that the ACL was cut while not damaging the PCL. The tibial tunnel was drilled retrograde from the ACL tibial insertion footprint to the outside of the medial tibia with a 28G needle. The needle was removed and then reinserted antegrade through the tibial tunnel to drill the femoral tunnel retrograde from the femoral ACL insertion footprint (Fig. 1E–F). The tendon graft was fed through the femoral and tibial tunnels, respectively, such that the cortical fixator was positioned on the outer cortex of the femur (Fig. 1G–H). At the tibial tunnel exit, the two ends of the tail tendon bundles were tied together with a basic square knot and then sutured to adjacent muscle (Fig. 1I). Another manual drawer test was performed to confirm that anterior–posterior translation was stabilized. Finally, the incision was closed with suture, analgesia was initiated (0.1 mg/kg buprenorphine), and the animal was returned to its cage following recovery from anesthesia.

Anterior–posterior drawer test

This procedure was adapted from Murata, *et al.*[24,25]. Both hindlimbs were harvested at four weeks postsurgery. The tibia was pinned to a small, rigid foam block by passing 25–27G needles transversely through the bone. Needles were then passed through the femur in a similar fashion. The tibia block was taped down to the horizontal shelf within a digital X-ray cabinet (Faxitron LX-60) and the knee was positioned at 90° of flexion (Fig. 2A). Sutures were wrapped around the needles in the femur and then attached to a 10 g weight that was hung off the edge of the Faxitron shelf via a pulley (Fig. 2A2). The 10 g force was applied in the tibial anterior direction and an X-ray image was acquired to define the posterior limit of motion. Subsequently, the weight was applied in the posterior direction of the tibia and an additional X-ray image was acquired to define the anterior limit of A–P drawer. The images were assembled as layers in the image analysis software (Fig. 2B). The distance between the anterior surface of the femoral condyle in the posteriorally- and anteriorally-displaced images was measured and normalized by the width of the tibial plateau in the sagittal plane to quantify anterior–posterior drawer.

Cryohistology

Hindlimbs were fixed in 10% neutral buffered formalin for 1–2 days, transferred to 30% sucrose in PBS overnight, and embedded in OCT. The knee was sectioned in the sagittal plane to capture longitudinal sections of the tibial and femoral tunnels. All sections were made from undecalcified joints using cryofilm 2C[14,2226–29], which maintains morphology of mineralized sections. The taped sections were secured to glass microscope slides using chitosan adhesive and rehydrated with 1× PBS prior to imaging.

Alkaline phosphatase staining

Alkaline phosphatase (AP) staining was performed using the Vector blue alkaline phosphatase substrate kit (Vector Labs) according to manufacturer protocols. The sections were incubated in the substrate solution for 15 minutes. The AP signal was imaged using a Cy5 filter (Ex: 640/30 and Em: 690/50).

Imaging

Three rounds of imaging were performed on each section. This sequence was possible because the cryofilm tape adheres to the tissue and allows for the coverslip to be removed between imaging steps without damaging the section. The order of imaging included: (1) fluorescent reporters and fluorescent mineralization labels, (2) alkaline phosphatase staining with DAPI counterstain, and (3) toluidine blue O (0.025% in dH_2O) staining.

Image analysis

All image analysis was conducted using Fiji (ImageJ, National Institutes of Health, Bethesda, MA) image analysis software {Schindelin:ty}. To measure the extent to which the *Gdf5-Cre*;tdTom$^+$ cells within the intact marrow expanded in response to the tunnel injury, the percent area of tdTom$^+$ signal was quantified from tissue sections by drawing a region of interest (ROI) that included all of the tibial epiphyseal bone marrow. An equivalent minimum threshold value was set for all samples and the positive pixels were divided by total pixels to calculate percent area.

To measure the extent to which *Gdf5-Cre*;tdTom$^+$ cells contribute to tunnel integration both in the epiphysis and metaphysis, we drew ROIs in these attachments as defined by alkaline phosphatase activity. We also drew ROIs within the native PCL enthesis within these sections. We then thresholded the DAPI channel to quantify individual nuclei and then measured the mean grayscale value from the tdTomato channel within each nucleus. An equivalent minimum threshold for tdTomato fluorescence was applied to quantify the number of nuclei that were tdTom positive. This number was divided by the total number of nuclei to calculate the percentage of *Gdf5-Cre*;tdTom$^+$ cells.

Statistics

The effect of ACL status (ACLT versus ACLR versus intact) on anterior–posterior drawer measurements were first compared via Kruskal–Wallis ($P < 0.05$) followed by Mann–Whitney U tests with significance level set to $P < 0.017$ to account for multiple comparisons. tdTom$^+$ percent area measurements in the bone marrow at 1-week postsurgery were compared between intact and ACLR knees via Mann–Whitney U tests with significance level set to $P < 0.05$. Finally, the percentage of tdTom$^+$ cells within the epiphyseal and metaphyseal attachments and native PCL were compared via Kruskal–Wallis ($P < 0.05$) followed by Mann–Whitney U tests with significance level set to $P < 0.017$ to account for multiple comparisons.

Results

ACL reconstruction restored

To assess knee stability following the ACL reconstruction healing process, reconstructed knees were compared with ACL-deficient (ACLT) and intact knees at 4 weeks postsurgery (Fig. 2). A–P translation in intact knees corresponded to 2.9 ± 1.6% of the tibial plateau compared with 22.8 ± 6.7% in ACLT knees ($P < 0.001$). After 4 weeks postreconstruction, A–P translation corresponded to 11.0 ± 6.7% in the ACLR knees, which equates to 58%

restoration of anterior–posterior stability compared with the ACLT group ($P = 0.012$) (Fig. 2C).

Gdf5-Cre;tdTom$^+$ cells in several tissues within the joint and epiphysis in the adult

Gdf5 is one of the key signaling factors expressed by interzone cells during joint development[20]. Progeny of Gdf5-expressing cells are found within mature tissues in the joint even into adulthood[22]. In our samples, we similarly saw *Gdf5-Cre*;tdTom$^+$ cells within the articular cartilage, cruciate ligaments (Fig. 3A1), collateral ligaments, synovium, and epiphysis. The cells in the epiphysis included osteoblasts overlaying a mineralization label in the trabecular bone (arrowhead in Fig. 3A2) and cells residing within the bone marrow (arrow in Fig. 3A2). The tail tendons of these mice, however, contained <1% *Gdf5-Cre*;tdTom$^+$ cells (Fig. 3B).

Gdf5-Cre;tdTom in response to the injury

At 1 week postsurgery, there was considerable expansion of *Gdf5-Cre*;tdTom$^+$ cells within the bone marrow (Fig. 4A1). The tdTom$^+$ percent area within the epiphyseal bone marrow increased to 54.1±12.1% from only 0.4±0.3% in the intact contralateral limb ($P < 0.05$). The leading front of the expanding cells approached the tendon graft interface (Fig. 4A3–4) where collagen fibers via second harmonic generation (SHG) imaging (yellow arrow in Fig. 4A5) containing tdTom$^+$ cells were juxtaposed with the denser and more aligned collagen fibers of the tendon graft. Similar to the intact limb (Fig. 3), there were higher number of *Gdf5-Cre*;tdTom$^+$ cells within the epiphysis than the metaphysis (Fig. S1, online only).

Gdf5-Cre;tdTom$^+$ cells give rise to zonal tendon-to-bone attachments within tunnels

The *Gdf5-Cre*;tdTom$^+$ bone marrow cells that interfaced with the tendon graft at 1 week postsurgery were now embedded between dense collagen fibers (Fig. 5A4 and yellow arrow in Fig. S1B (online only)) spanning an organized tidemark (yellow demeclocycline label denoted by white arrow in Fig. 5A4–6) separating unmineralized and mineralized fibrocartilage (* in Fig. 5A3) of zonal attachments. Alkaline phosphatase facilitates the deposition of mineral and is concentrated near the tidemark in the normal enthesis[14]. Alkaline phosphatase was concentrated near the demeclocycline tidemark in the bone tunnel attachments as well (Fig. 5A6). We quantified the number of *Gdf5-Cre*;tdTom$^+$ cells within the alkaline phosphatase regions and found that 55.4 ± 18.9% of cells within the epiphyseal attachments were tdTom$^+$ compared with only 1.6 ± 1.6% of cells in the metaphyseal attachments ($P = 0.009$). This labeling efficiency compared with 77.2 ± 8.2% in the nearby posterior cruciate ligament entheses (Fig. 5B). The collagen fibers of the attachments were anchored to the adjacent bone which surrounded the tunnel at 4 weeks. In contrast, very little trabecular bone was found at the graft interface at 1 week postsurgery (Fig. 4A1). Attachments with all of these attributes were found within both tunnels for all mice at four weeks post-reconstruction.

Gdf5-Cre;tdTom$^+$ cells revitalized the tendon graft

At one week following reconstruction, the tendon graft was hypocellular both within the bone tunnels (Fig. 4A1, 4) and the joint space (Fig. 6A), with the majority of nuclei in the

graft existing near the graft surface (white arrow). By 4 weeks, a large number of *Gdf5-Cre*;tdTom^{+} cells were found within the tendon graft, especially in the regions of the graft within the bone tunnels (Figs. 5A4 and 5B, and Fig. S1B1 (online only)). In contrast, the graft tissue within the central region of the joint remained largely acellular at 4 weeks (Fig. 6B). The majority of *Gdf5-Cre*;tdTom^{+} cells that infiltrated the graft within the joint space were adjacent to the tunnel entrances on both the femur and tibia (yellow arrow in Fig. 6B).

Discussion

Two events are crucial to successful biological repair following ACL reconstruction: (1) cells need to revitalize the graft, as resident cells within the graft frequently die following reconstruction[9–13], and (2) the soft tissue graft needs to integrate with the adjacent bone in the tunnels through the formation of zonal attachments[6,30]. We used our murine ACL reconstruction model to monitor graft revitalization following reconstruction and the formation of mineralized attachments within the bone tunnels (Figs. 4–6). We performed these procedures in *Gdf5-Cre*;R26R-tdTomato mice because the progeny of Gdf5-expressing embryonic cells give rise to mesenchymal cells within the joint and epiphysis but not the tail tendons, permitting us to monitor infiltration of surrounding resident cells into the unlabeled tail tendon (Fig. 3B). We found in this model that cells from outside the graft within the bone marrow are the primary cell population that contributes to tunnel integration through the production of zonal tendon-to-bone insertion sites (Figs. 4 and 5), while cells within the synovial lining revitalize the graft midsubstance within the joint space (Fig. 6).

Gdf5 expression reduces dramatically after birth[21] yet mesenchymal cells within the epiphyseal bone marrow persist into adulthood. Furthermore, we found that *Gdf5-Cre*;tdTom^{+} cells only contributed to epiphyseal attachments and not attachments within metaphyseal regions of the bone tunnel (Fig. 5B and Fig. S1 (online only)), suggesting that Gdf5 was not activated in these cells during the repair process. Therefore, the implication of this work is that a self-renewing stem/progenitor population derived from an embryonic cell population persists into adulthood. This stem/progenitor population then activates in response to the ACL reconstruction injury to contribute to zonal tendon-to-bone attachments in the tunnel integration process.

The coordinated events of zonal enthesis formation are well characterized in the developing animal during embryogenesis and postnatal growth. Enthesis progenitors expressing Gdf5[14,22,23], among other markers[31–33], go on to assemble collagen fibers that are anchored to the underlying cartilage template, surround these fibers with a proteoglycan-rich matrix (i.e., unmineralized fibrocartilage), and then finally mineralize a portion of this fibrocartilage to create the zonal enthesis. In this study, we found that adult cells from a Gdf5 origin within the epiphyseal bone marrow had the potential to assemble zonal attachments within the bone tunnel following ACL reconstruction. While not as organized, these attachments displayed aspects of a normal zonal enthesis, with collagen fibers spanning across an organized tidemark (Fig. 5A5), alkaline phosphatase activity adjacent to this tidemark (Fig. 5A6), and proteoglycans within the fibrocartilage (purple stain in Fig. 5A3). Unlike direct tendon-to-bone repair, which typically results in disorganized scar, the ACL reconstruction procedure yields zonal tendon-to-bone attachments, even in murine models as used in this study.

Therefore, the vast genetic tools available in various mouse models can be used to better understand the molecular mechanisms that regulate zonal tendon-to-bone repair in the adult.

There were key aspects of the zonal attachment formation in the ACL reconstruction model that are quite distinct from normal development. Even though the adult bone marrow mesenchymal progenitor cells that give rise to these attachments come from a GDF5 lineage, they are quite different from the interzone-derived cells that give rise to the normal ACL enthesis. The *Gdf5-Cre*;tdTom$^+$ cells that respond to the bone tunnel injury give rise to both the mineralized attachments in the tunnel as well as the contiguous bone adjacent to the attachment. Therefore, there is either a fate decision that is made by a common progenitor, or there is a heterogeneous progenitor pool with some cells serving as osteoprogenitors giving rise to trabecular bone and others as chondroprogenitors giving rise to the zonal attachments. Defining that a heterogeneous progenitor pool exists versus identifying the mechanisms that drive fate decisions from a common progenitor would provide novel cell and molecular targets to enhance or accelerate the repair response.

This study is not without limitations. First, we were unable to fully restore the anterior stability of the knee following the reconstruction procedure. This was primarily because the tunnels could not be drilled perfectly on the native footprints of the ACL without fracturing the epiphyses, particularly in the tibia. Therefore, this instability could dictate the cell response within the graft and the tunnel integration process. Second, the *Gdf5-Cre* model is not inducible and therefore the timing of recombination cannot be easily controlled. However, Gdf5 expression in the joint is mostly restricted to embryonic time points[21] and *Gdf5-Cre*;tdTom$^+$ cells were not found in the metaphyses, even after injury (Fig. 5B and Fig. S1 (online only)). Therefore, it is likely that the recombination to drive tdTomato expression occurred during these early ages and not during the injury response. Finally, the radiographic-based anterior drawer test was limited in that we did not control rotation of the femur during the test and viscoelastic properties could not be measured. However, our lab has recently developed an anterior–posterior drawer test on a mechanical testing machine so viscoelastic properties can now be measured[19]. Nevertheless, the radiographic method yielded percent changes in displacement that fell within previous reports for anterior drawer tests in ACL-deficient human knees[34,35]. Additionally, the radiographic methods provides labs without access to sophisticated mechanical testing machines a procedure to measure anterior–posterior stability of the knee.

The mechanisms that drive the formation of the enthesis during growth and development may be similar to the mechanisms that regulate the formation of tendon-to-bone attachments within the bone tunnels, especially since these attachments have mineralized fibrocartilage with an organized tidemark. Since the stem/progenitor population that gives rise to this response is likely a self-renewing population from an embryologic origin, it indicates that this is a potent cell population that could be used to improve tendon-to-bone repair. Murine models of ACL reconstruction provide a platform where key cell signaling pathways can be targeted genetically and pharmacologically to modulate the tunnel integration process. Future studies will work to modulate the GDF5-origin cells that contribute to tunnel integration to better understand the molecular mechanisms driving zonal tendon-to-bone repair.

Supplementary Material

Refer to Web version on PubMed Central for supplementary material.

Acknowledgements

The authors would like to thank Dr. David Kingsley for graciously providing the *Gdf5-Cre* mice. This work was supported by NIH Grant K99/R00 AR067283 (NAD) and DOD Grant W81XWH-15-1-0371. (DJA).

References

1. Praemer A, Furner S, and Rice DP 1999, Musculoskeletal conditions in the United States American Academy of Orthopaedic Surgeons, Rosemont, IL.
2. Awad HA 2012, Prospects of Tendon Tissue Engineering in Sports Medicine. Dtsch Z Sportmed, 2012, 132–5.
3. Calejo I, Costa-Almeida R, and Gomes ME 2019, Cellular Complexity at the Interface: Challenges in Enthesis Tissue Engineering. Adv. Exp. Med. Biol, 1144, 71–90. [PubMed: 30632116]
4. Mather RCI, Koenig L, Kocher MS, et al. 2013, Societal and Economic Impact of Anterior Cruciate Ligament Tears. J Bone Joint Surg, 95A, 1751–9.
5. Barber-Westin SD, and Noyes FR 2011, Factors Used to Determine Return to Unrestricted Sports Activities After Anterior Cruciate Ligament Reconstruction. Arthroscopy, 27, 1697–705. [PubMed: 22137326]
6. Deehan DJ, and Cawston TE 2005, The biology of integration of the anterior cruciate ligament. J Bone Joint Surg [Br], 87, 889–95.
7. Kobayashi M, Watanabe N, Oshima Y, Kajikawa Y, Kawata M, and Kubo T 2005, The fate of host and graft cells in early healing of bone tunnel after tendon graft. Am J Sports Med, 33, 1892–7. [PubMed: 16157856]
8. Ekdahl M, Wang JH-C, Ronga M, and Fu FH 2008, Graft healing in anterior cruciate ligament reconstruction. Knee Surg Sports Traumatol Art, 16, 935–47.
9. Daniel DM, Akeson WH, and O'Connor JJ 1990, Knee ligaments. Raven Pr.
10. Rougraff BT, and Shelbourne KD 1999, Early histologic appearance of human patellar tendon autografts used for anterior cruciate ligament reconstruction. Knee Surg Sports Traumatol Art, 7, 1–6.
11. Rougraff B, Shelbourne KD, Gerth PK, and Warner J 1993, Arthroscopic and histologic analysis of human patellar tendon autografts used for anterior cruciate ligament reconstruction. Am J Sports Med, 21, 277–84. [PubMed: 8465925]
12. Claes S, Verdonk P, Forsyth R, and Bellemans J 2011, The "Ligamentization" Process in Anterior Cruciate Ligament Reconstruction. Am J Sports Med, 39, 2476–83. [PubMed: 21515806]
13. Takahashi T, Kondo E, Yasuda K, et al. 2016, Effects of Remnant Tissue Preservation on the Tendon Graft in Anterior Cruciate Ligament Reconstruction: A Biomechanical and Histological Study. Am J Sports Med, 44, 1708–16. [PubMed: 27159314]
14. Dyment NA, Breidenbach AP, Schwartz AG, et al. 2015, Gdf5 progenitors give rise to fibrocartilage cells that mineralize via hedgehog signaling to form the zonal enthesis. Dev Biol, 405, 96–107. [PubMed: 26141957]
15. Bachy M, Sherifi I, Zadegan F, Petite H, Vialle R, and Hannouche D 2016, Allograft integration in a rabbit transgenic model for anterior cruciate ligament reconstruction. Orthop Traumatol Surg Res, 102, 189–95. [PubMed: 26775085]
16. Deng XH, Lebaschi A, Camp CL, et al. 2018, Expression of Signaling Molecules Involved in Embryonic Development of the Insertion Site Is Inadequate for Reformation of the Native Enthesis: Evaluation in a Novel Murine ACL Reconstruction Model. J Bone Joint Surg, 100, e102. [PubMed: 30063598]

17. Lebaschi A, Deng XH, Coleman NW, et al. 2017, Restriction of Postoperative Joint Loading in a Murine Model of Anterior Cruciate Ligament Reconstruction: Botulinum Toxin Paralysis and External Fixation. J Knee Surg, 30, 687–93. [PubMed: 27907934]
18. Camp CL, Lebaschi A, Cong G-T, et al. 2017, Timing of Postoperative Mechanical Loading Affects Healing Following Anterior Cruciate Ligament Reconstruction: Analysis in a Murine Model. J Bone Joint Surg Am, 99, 1382–91. [PubMed: 28816898]
19. Kamalitdinov TB, Fujino K, Shetye SS, et al. 2019, Amplifying Bone Marrow Progenitors Expressing α-Smooth Muscle Actin Produce Zonal Insertion Sites During Tendon-to-Bone Repair. J Orthop Res, 24, 182.
20. Koyama E, Shibukawa Y, Nagayama M, et al. 2008, A distinct cohort of progenitor cells participates in synovial joint and articular cartilage formation during mouse limb skeletogenesis. Dev Biol, 316, 62–73. [PubMed: 18295755]
21. Pregizer SK, Kiapour AM, Young M, et al. 2018, Impact of broad regulatory regions on Gdf5 expression and function in knee development and susceptibility to osteoarthritis. Annals of the Rheumatic Diseases, 77, 450–0. [PubMed: 29311146]
22. Dyment NA, Hagiwara Y, Matthews BG, Li Y, Kalajzic I, and Rowe DW 2014, Lineage Tracing of Resident Tendon Progenitor Cells during Growth and Natural Healing Asakura A, (ed.). PLoS ONE, 9, e96113–12. [PubMed: 24759953]
23. Rountree RB, Schoor M, Chen H, et al. 2004, BMP Receptor Signaling Is Required for Postnatal Maintenance of Articular Cartilage Lee Niswander, (ed.). PLoS Biol, 2, e355–13. [PubMed: 15492776]
24. Murata K, Kanemura N, Kokubun T, et al. 2017, Controlling joint instability delays the degeneration of articular cartilage in a rat model. Osteoarthritis and Cartilage, 25, 297–308. [PubMed: 27756697]
25. Murata K, Kokubun T, Morishita Y, et al. 2018, Controlling Abnormal Joint Movement Inhibits Response of Osteophyte Formation. Cartilage, 9, 391–401. [PubMed: 28397529]
26. Dyment NA, Jiang X, Chen L, et al. 2016, High-Throughput, Multi-Image Cryohistology of Mineralized Tissues. J Vis Exp, e54468–8.
27. Dyment NA, Hagiwara Y, Jiang X, Huang J, Adams DJ, and Rowe DW 2015, Response of knee fibrocartilage to joint destabilization. Osteoarthritis and Cartilage, 23, 1–11. [PubMed: 25219671]
28. Dyment NA, Liu C-F, Kazemi N, et al. 2013, The Paratenon Contributes to Scleraxis-Expressing Cells during Patellar Tendon Healing Mezey E, (ed.). PLoS ONE, 8, e59944–11. [PubMed: 23555841]
29. Zhang J, Dyment NA, Rowe DW, et al. 2016, Ectopic mineralization of cartilage and collagen-rich tendons and ligaments in Enpp1asj-2J mice. Oncotarget, 7, 12000–9. [PubMed: 26910915]
30. Bedi A, Kawamura S, Ying L, and Rodeo SA 2009, Differences in tendon graft healing between the intra-articular and extra-articular ends of a bone tunnel. HSS Jrnl, 5, 51–7.
31. Blitz E, Sharir A, Akiyama H, and Zelzer E 2013, Tendon-bone attachment unit is formed modularly by a distinct pool of Scx- and Sox9-positive progenitors. Development, 140, 2680–90. [PubMed: 23720048]
32. Sugimoto Y, Takimoto A, Akiyama H, et al. 2013, Scx+/Sox9+ progenitors contribute to the establishment of the junction between cartilage and tendon/ligament. Development, 140, 2280–8. [PubMed: 23615282]
33. Soeda T, Deng JM, de Crombrugghe B, Behringer RR, Nakamura T, and Akiyama H 2010, Sox9-expressing precursors are the cellular origin of the cruciate ligament of the knee joint and the limb tendons. Genesis, 48, 635–44. [PubMed: 20806356]
34. Furman W, Marshall JL, and Girgis FG 1976, The anterior cruciate ligament. A functional analysis based on postmortem studies. J Bone Joint Surg, 58, 179–85. [PubMed: 1254621]
35. Hsieh HH, and Walker PS 1976, Stabilizing mechanisms of the loaded and unloaded knee joint. J Bone Joint Surg, 58, 87–93. [PubMed: 946171]

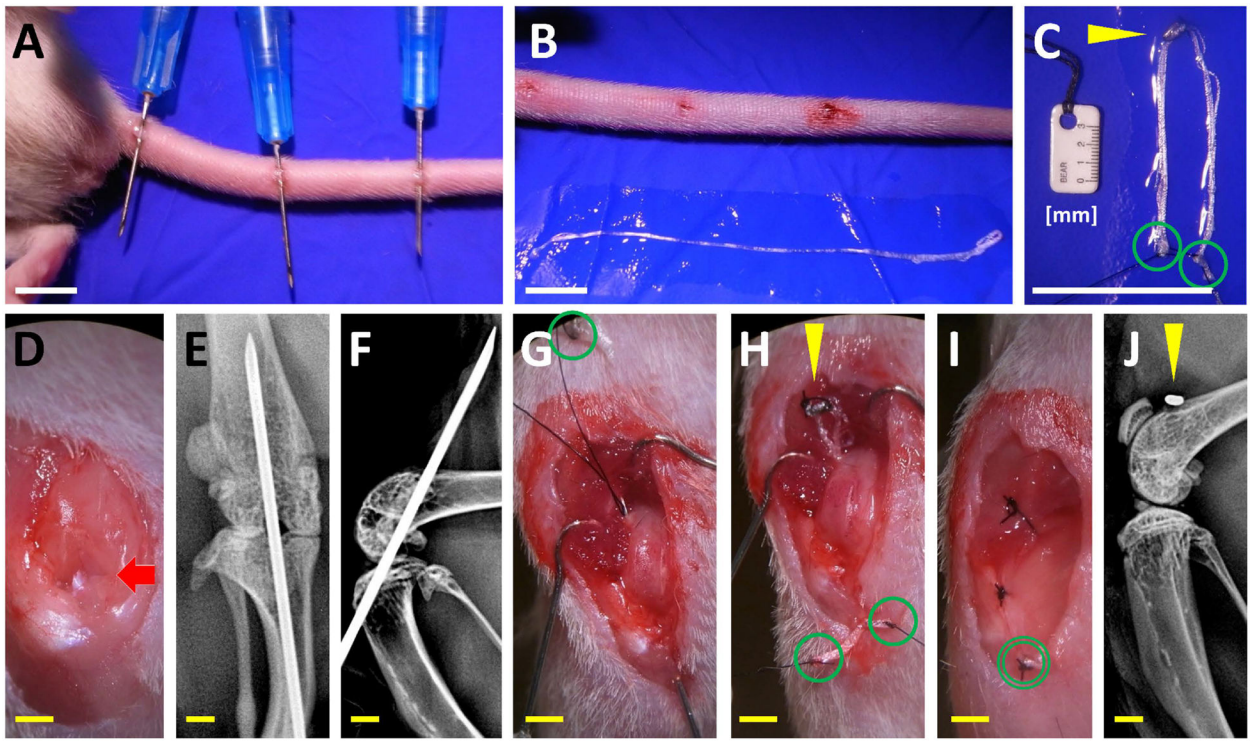

Figure 1.

Murine ACL reconstruction procedure using tail tendon autograft. Three incisions along the length of the tail (A) were used to isolate segments of tail tendons (B). These tendon bundles were secured with suture (green circles in C) and a cortical fixator was applied to the midpoint of the bundle (yellow arrowhead in C). The ACL (red arrow in D) was accessed using an anteromedial approach. The tibial and femoral tunnels were drilled (E–F) and the graft was fed into the tunnels from the femur (G) and out the tibia (H). The cortical fixator (yellow arrowhead in H and J) provided fixation on the femur while the tail tendon bundle was tied and sutured to the adjacent muscle (I) to provide fixation on the tibia. White scale bars in top row are 10 mm while yellow scale bars in bottom row are 1 millimeter.

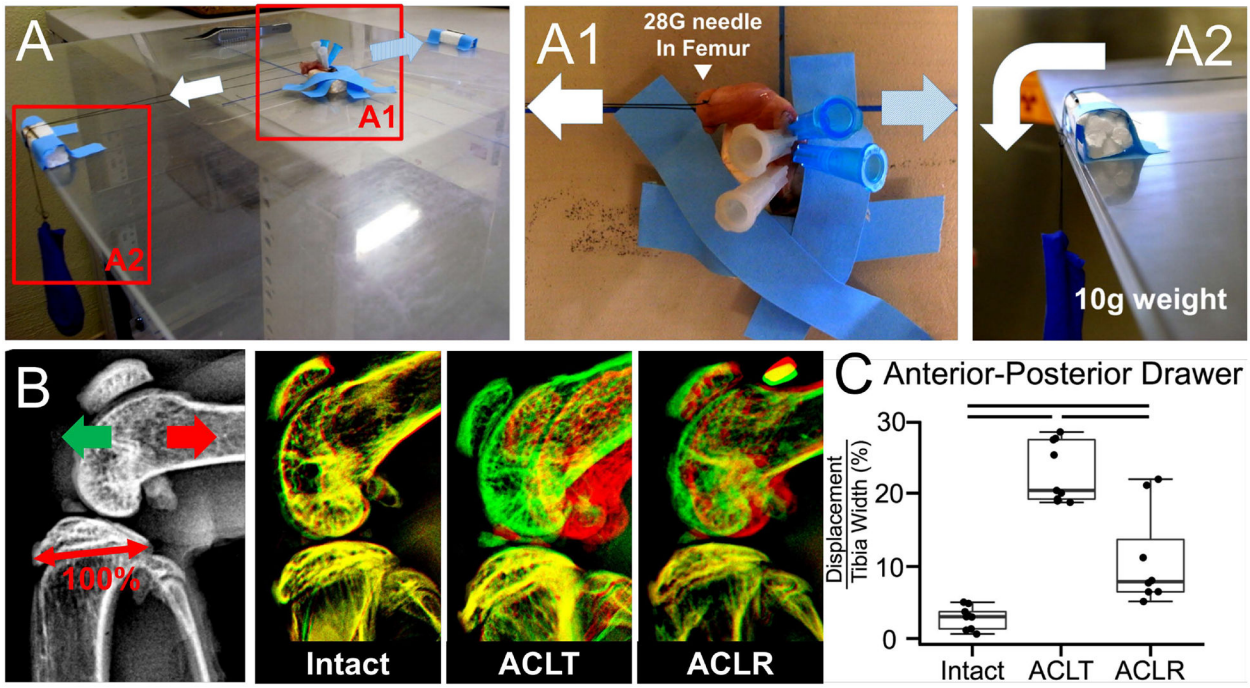

Figure 2.

Reconstruction procedure restores 58% of anterior–posterior stability of knee joint. At 4 weeks postsurgery, the limb was harvested and the tibia was pinned to a foam block using needles and taped to the shelf of a digital X-ray cabinet (A). A needle was passed through the femur (A1) and then suture was tied to this needle on one end and to a 10-g weight on the other end (A2). The weight was applied in the anterior (light blue arrow in A1) and posterior (white arrow in A1) directions relative to the tibia, acquiring a radiograph at each position. The two images were overlaid (B) and the displacement of the femur from anterior to posterior images was measured and normalized to the width of the tibial plateau (denoted as 100% in B). Measurements are reported in (C). Bars indicate $P < 0.017$. Intact knee ($n = 9$), ACLT,ACL-deficient knee ($n = 9$), or ACLR, ACL reconstructed knee ($n = 8$).

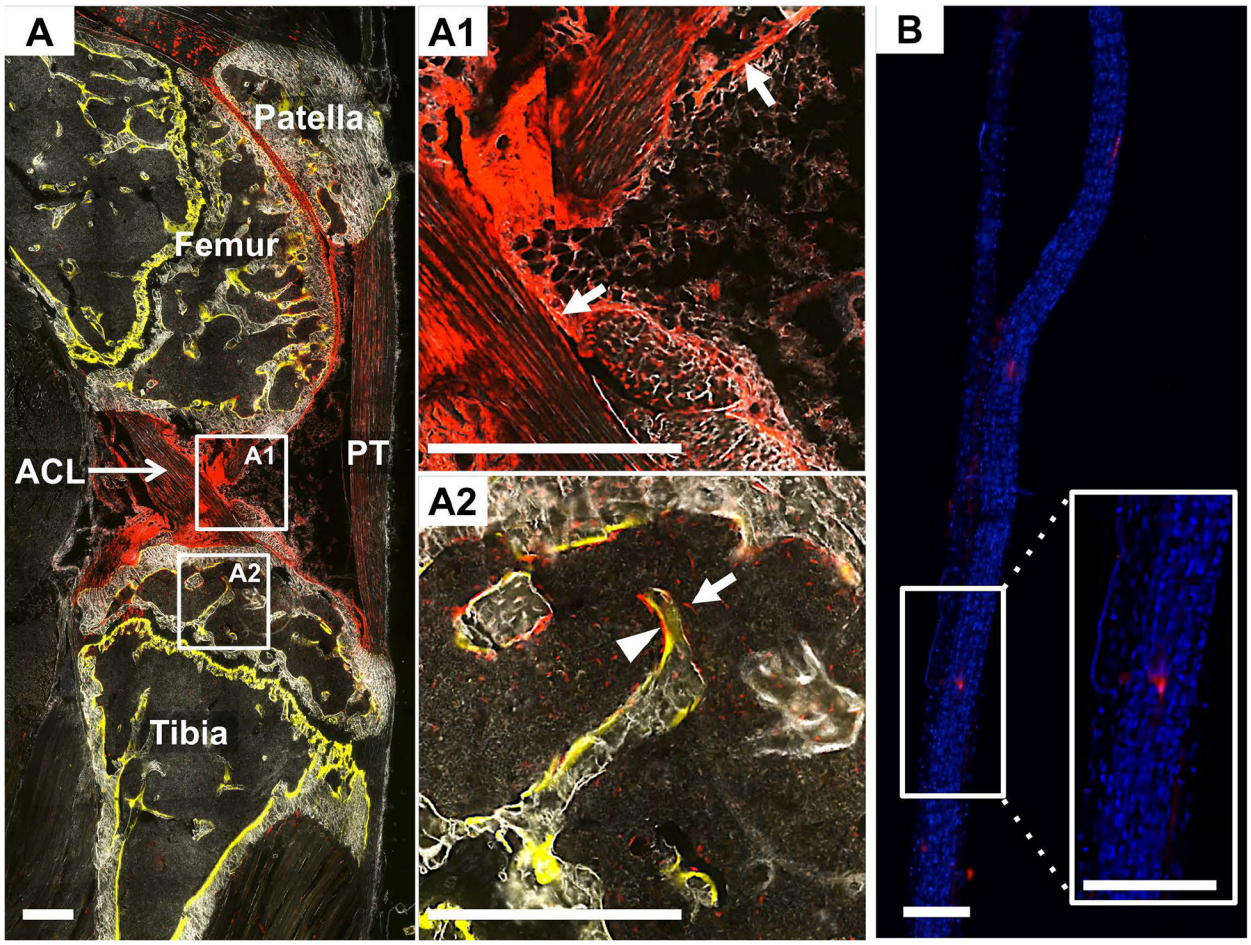

Figure 3.

tdTom^{+} cells exist within the knee but not tail tendons of *Gdf5-Cre*;R26R-tdTomato mice. The intact contralateral knee from an ACLR mouse that received demeclocycline injection (yellow in A) the day prior to sacrifice. *Gdf5-Cre*;tdTom^{+} cells exist within the synovial lining (white arrows in A1), cruciate ligaments (A1), epiphyseal bone (arrow head in A2), and bone marrow (arrow in A2). Conversely, the tail tendons from these mice possess very few *Gdf5-Cre*;tdTom^{+} cells (B). Scale bars: 200 μm.

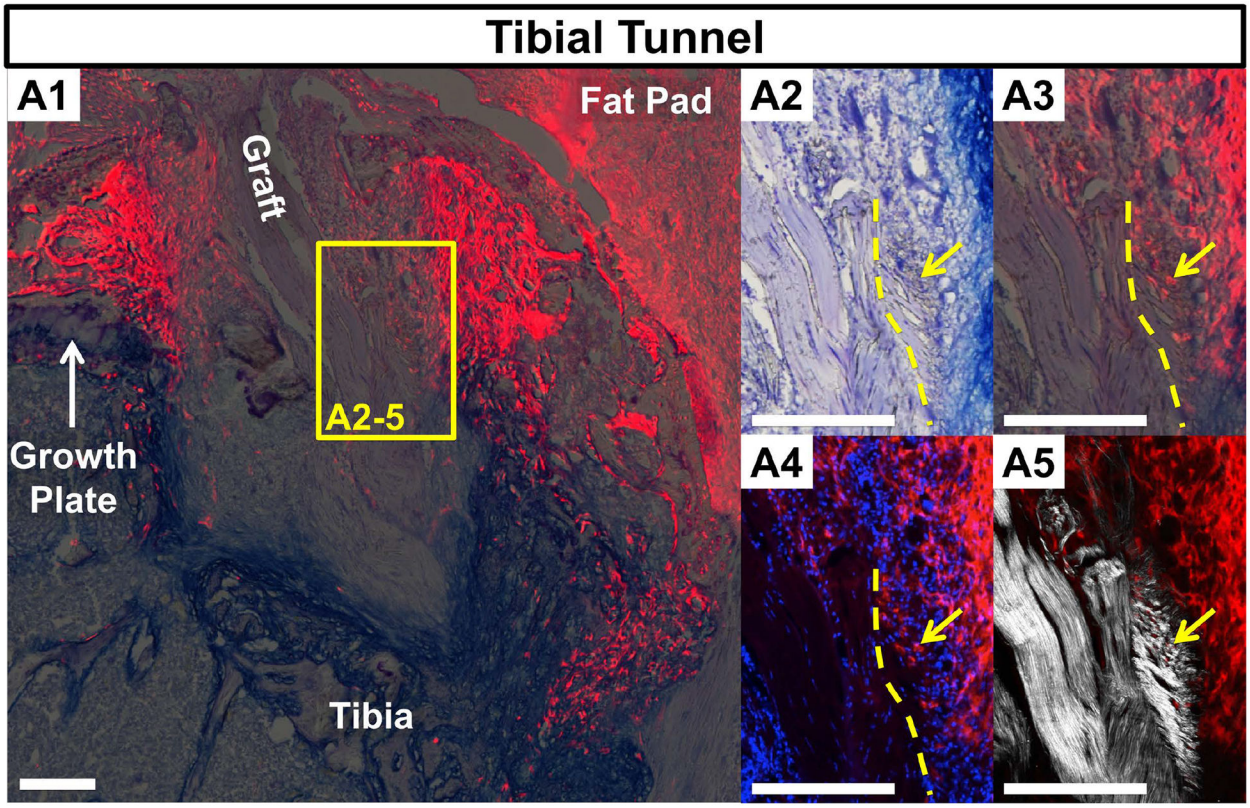

Figure 4.

Expansion of *Gdf5-Cre*;tdTom^{+} epiphyseal bone marrow cells and early attachments at 1 week postsurgery. (A) Tibial tunnel is shown with tendon graft in the center flanked by expanding tdTom^{+} bone marrow population. Panels A2–5 demonstrate early attachments at the interface of the graft with the marrow space. (A2) toluidine blue O stain, (A3) tdTom channel (red) overlaid onto toluidine blue image, (A4) tdTom channel with DAPI counterstain, and (A5) collagen SHG with tdTom channel. Dotted lines denote interface between dense collagen of graft and looser collagen containing tdTom^{+} cells (yellow arrow). Scale bars: 200 μm.

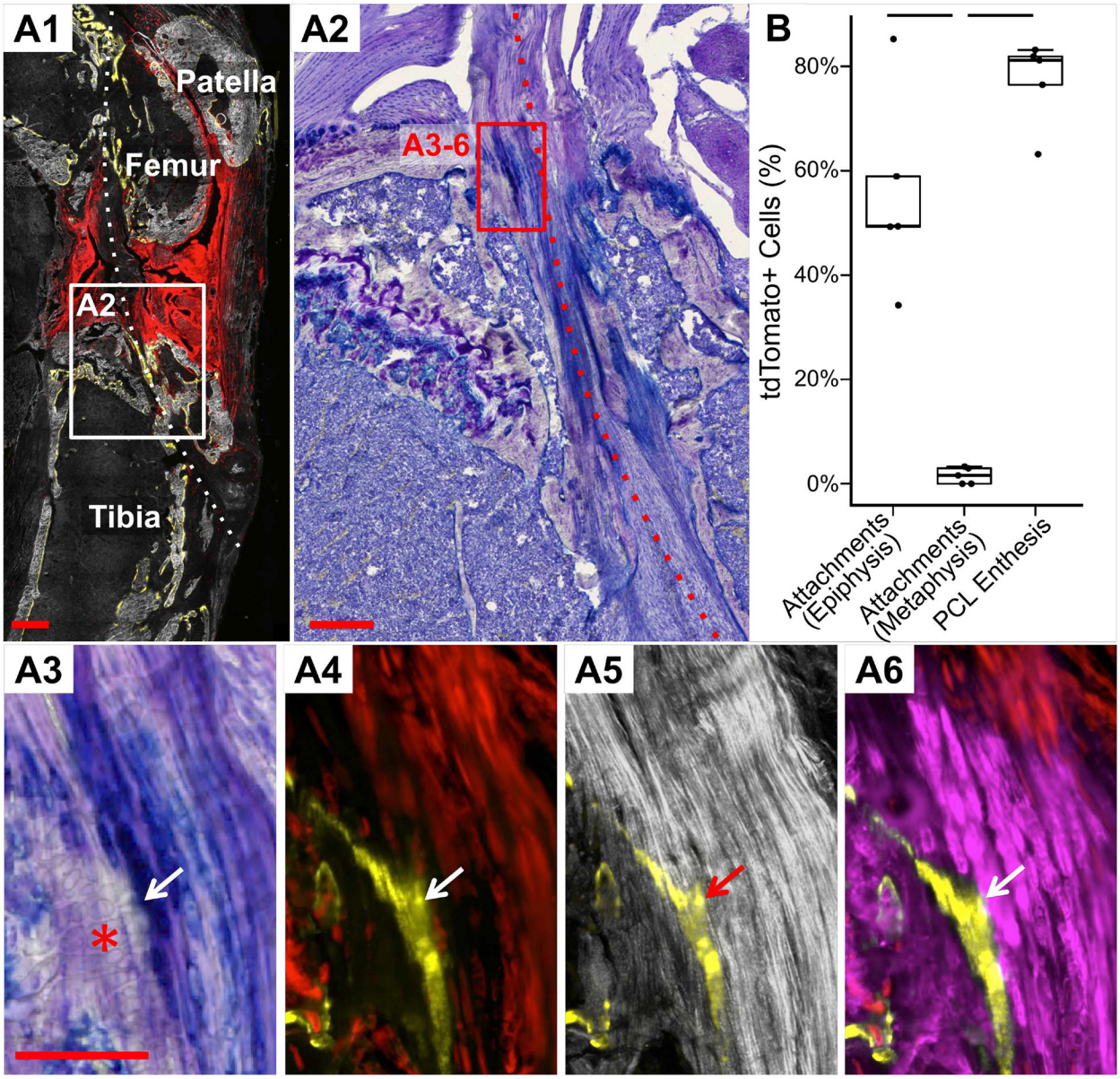

Figure 5.

Gdf5-Cre;tdTom^{+} cells produce mineralized attachments in the epiphyseal regions of the bone tunnels. (A1) Image of entire knee joint with dotted line denoting tunnel path at 4 weeks postsurgery. (A2) Toluidine blue stained image of tibial tunnel. Panels A3–6 demonstrate zonal attachment at the entrance to the tibial tunnel. (A3) Toluidine blue O image, (A4) tdTom channel (red) with demeclocycline label (yellow), (A5) collagen SHG with demeclocycline, and (A6) tdTom channel with demeclocycline and alkaline phosphatase activity (magenta). Arrows denote yellow demeclocycline tidemark. * denotes mineralized fibrocartilage. Scale bar: 200 μm. (B) quantification of the percentage of tdTom $^{+}$ cells within alkaline phosphatase regions of the epiphyseal and metaphyseal attachments along with the native PCL entheses. Bars indicate $P < 0.017$.

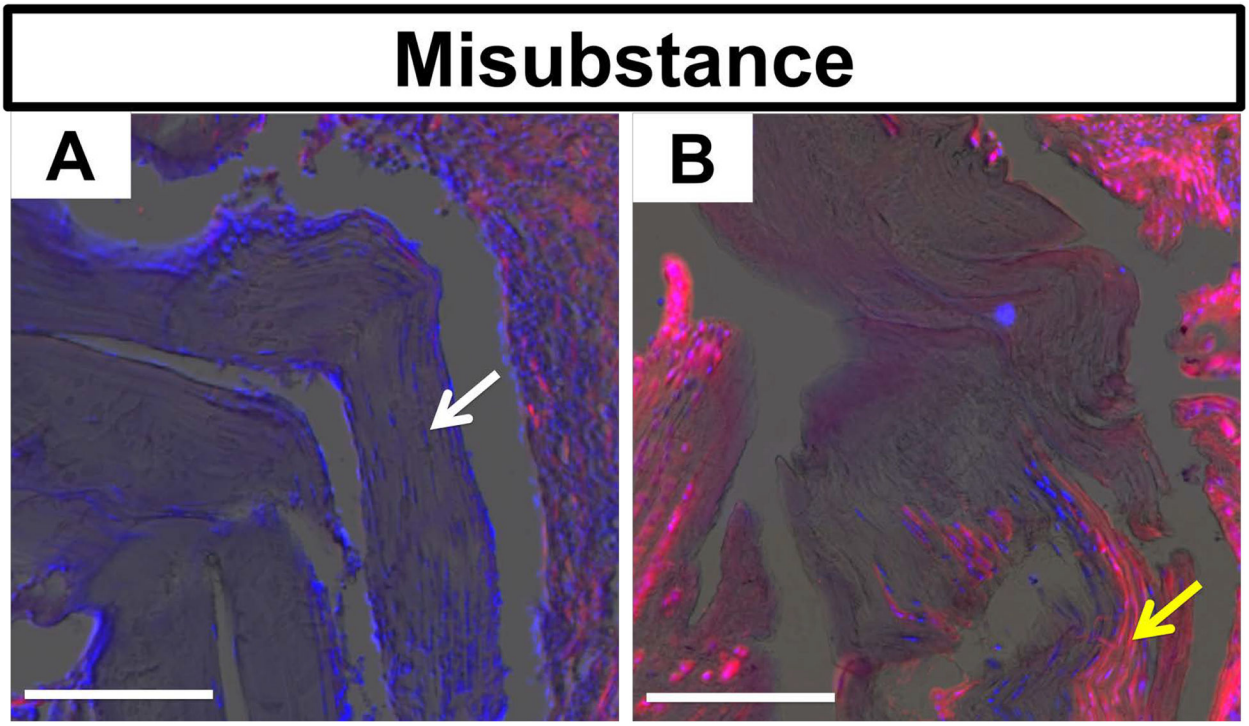

Figure 6.

Cell death occurred within the graft midsubstance and there was limited cell repopulation. Images of the tendon graft within joint space at 1 week (A) and 4 weeks (B) postsurgery. Images are of tdTom channel (red) with DAPI counterstain (blue) overlaid on toluidine blue O image. Graft at 1 week possesses live cells near the surface of the graft (white arrow), while the graft was mostly acellular at 4 weeks with cellular portions coming from repopulating *Gdf5-Cre*;tdTom^{+} cells (yellow arrow) near the entrance to the bone tunnel. Scale bars: 200 μm.